Evaluation of Machine Learning Methods for Prediction of Multiphase Production Rates

Dr. Anton Gryzlov, Liliya Mironova, Dr. Sergey Safonov and Dr. Muhammad Arsalan

Abstract /

Multiphase flow metering is an important tool for production monitoring and optimization. Although there are many technologies available on the market, the existing multiphase meters are only accurate to a certain extent and generally are expensive to purchase and maintain.

Use of virtual flow meters are a low-cost alternative to conventional production monitoring tools, which relies on mathematical modeling rather than the use of hardware instrumentation. Supported by the availability of the data from different sensors and production history, the development of different virtual flow metering systems has become a focal point for many companies.

This article discusses the importance of flow modeling for virtual flow metering. In addition, main data-driven algorithms are introduced for the analysis of several dynamic production data sets. Artificial neural networks (ANN), together with advanced machine learning methods, such as the gated recurrent unit (GRU) and extreme gradient boosting (XGBoost), have been considered as possible candidates for virtual flow metering. The obtained results indicate that the machine learning algorithms estimate oil, gas, and water rates with acceptable accuracy. The feasibility of the data-driven virtual flow metering approach for continuous production monitoring purposes has been demonstrated via a series of simulation-based cases. Among the used algorithms, the deep learning methods provided the most accurate results combined with reasonable time for model training.

Introduction

Knowledge of multiphase flow rates from each well in a production network is an important component for optimal management of oil and gas reservoirs. The information on the multiphase rates of produced oil, gas, and water can significantly facilitate decision making on production stimulation, optimization of field operations, and control. Additionally, continuous production monitoring provides critical information for reservoir history matching and helps to estimate the hydrocarbon reserves.

Currently, the industry offers two solutions: a test separator or a multiphase flow meter. Both of these methods have certain disadvantages. The test separators are bulky, provide a slow response to rapid flow changes, and require sufficient installation space. The multiphase meters are generally expensive and require regular maintenance. More importantly, no technology exists that provides measurements in all possible flow conditions with acceptable accuracy in a single multiphase meter.

To overcome these challenges, methods of indirect flow rate calculation have been introduced. The technique, called virtual flow metering — also known as soft sensing, data validation, and reconciliation, or soft multiphase flow metering — has been widely used to estimate the multiphase rates from conventional sensors, such as downhole pressure and temperature gauges. All of these methods take advantage of using instrumentation, which is already available in the well, thereby becoming a cheaper alternative to the regular multiphase flow meters. Virtual flow metering uses all the data available from the sensors to calculate the flow rates by applying mathematical modeling. This computational algorithm can be based on the rigorous first principle equations describing the flow, or be represented by some data-driven operator establishing the hidden relationship between available measurements and target flow rates. The complete classification of all virtual flow meter methods is available[1].

A data-driven approach does not require any background information on underlying physics. Instead, it is based on the available data and uses some machine learning techniques, which build predictive models directly from the data available. Contrary to other methods, the data-driven virtual flow meter is very easy to set up and deploy, however, these methods are normally well specific and fail to perform satisfactory if the conditions are outside a certain data range. There are multiple examples where machine learning and data analytic methods were used as the predictors for multiphase production technology[2-4]. The popularity of machine learning has risen dramatically, due to the recent developments of neural networks, improvement of hardware resources, and exponential growth of data available from an oil field. All of these factors helped to drastically increase the resolution and predictive capabilities of computational models under development.

The goal of the present article is to demonstrate the workflow and results of implementing different types of a

data-driven virtual flow meter, such as a basic artificial neural network (ANN), advanced gated recurrent unit (GRU), and a gradient boosting method. Such information is essential to increase the understanding of which machine learning method is more suitable to certain conditions or data. The analysis includes a discussion on how noisy data needs to be processed, which is an important issue for real-life applications.

Virtual Flow Metering: Flow Modeling

The critical component of any virtual flow metering system is the flow model, which relates observed quantities, i.e., measurements, to the hidden ones, i.e., rates. As it has been previously mentioned, the flow models can be either data-driven or physics-driven, the latter is also subdivided into steady-state and transient types. Moreover, a different classification is proposed here, where the virtual measurements are performed either in an open or closed loop paradigm.

There are generic challenges associated with both approaches; the data from the field is never perfect, and there is noise contamination or systematic biases that need to be considered before either of the virtual flow meter approaches can be put into practice. In addition, for the physics-based virtual flow meter, the quality of the first principle models is essential. Normally, the simplified approach is used, where the multiphase flow is treated as 1D, which is obtained from cross-sectional averaging of the conservative equations and supplementing it with flow regime independent closure terms[5]. These models follow the main conservation laws, although they rely heavily on the empirical correlations obtained from the lab experiments[6]. By default, all of these models are only rough approximations of reality and never describe the production system perfectly. As the result, accounting model error and measurement noise is an important part of a virtual flow meter workflow, which can be done in a closed loop manner, Fig. 1.

In this approach, the predictions of the model are compared with the measurements via data assimilation algorithms. Measurements include information from different sensors, which provide some flow-related quantity, which is not one of direct interest. Consequently, there is a strong connection between the unknown flow rates and the readings from these sensors. Some measurements are more easily obtained at the surface conditions rather than downhole, although the latter are usually accessible only at a few locations. On the other hand, the physical flow model can estimate the multiphase flow rate if it is properly initialized. Moreover, due to different simplifications previously mentioned and uncertainty in the initial conditions, the resulting predictions will deviate from real values. Therefore, these two sources of information, the model and the measurements, cannot be used for the accurate prediction of multiphase rates if used independently.

Data assimilation is the process that integrates the measurements from the actual sensors and the simulated outputs of the flow model in an intelligent way, which is a mismatch between predicted and measured data. One can see two different approaches for incorporating

Fig. 1 *The closed loop virtual flow meter workflow.*

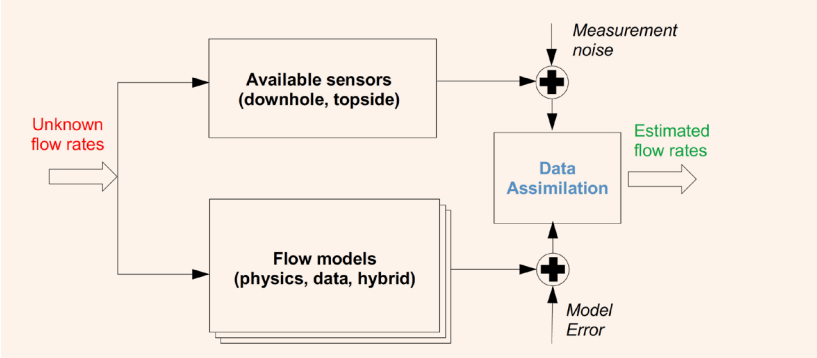

measurement data into the flow model: (1) variation data assimilation, which is based on the minimization of a cost function within a certain time interval[7], and (2) filtering, where the state of the system is updated every instant when new data become available[8]. While the variational data assimilation tries to iterate state variables to fit the measurements over a certain time window (also called an assimilation window), the filtering algorithms act in real-time, integrating measurements at the current time step into the model.

Note that here the outputs of the model and measurements can be completely different, as the closed loop virtual flow meter provides model-based predictions of both measured and unmeasured quantities. For that purpose, the multiphase flow model of the system should be described theoretically, allowing unequivocal predictions of dynamic variables (system output) with a given model input. The model does not necessarily need to be only physics-based; a data-driven approach could be used in this paradigm as well.

The use of dynamic mode decomposition[9] is especially attractive for this purpose, as it offers a purely explicit approximation of dynamics in state space representation. In addition, one could consider the application of the hybrid methods, where the first principle knowledge is somehow embedded into the machine learning algorithm to constrain the uncertainties and improve predictive capabilities. Examples of closed loop virtual flow metering can be found in Lorentzen et al. (2016)[10] and Gryzlov (2009)[11].

The open loop virtual flow meter is based on the direct use of a function that maps the input measurements to the target rates. This mapping is also referred to as training (or calibration), as it adjusts the parameters of this function to match the known input-output pairs. Once the model is prepared it can be immediately used by feeding it with newly available measurements.

The data-driven methods are especially suited for open loop applications. For the neural networks, for instance, the training corresponds to the adjustment of model weights and biases connecting neurons. The optimal model parameters are formulated as the minimal difference between the prediction of the algorithm and

the true flow rates.

Although it may look similar, the formulation of the cost function constitutes the essential difference from the closed loop approach, where the model predictions are compared to all possible measurements, not just the output rates, which are not normally available. In addition, in the open loop framework, the model is tuned only once, before the application, while the closed loop approach corrects its behavior every time if there is a significant deviation of the model from the measurements.

The distinction between these two approaches can be formulated differently. While data-driven methods look at the best mathematical functions, which relate input and output measurements, the closed loop approach tends to adjust the behavior of the model in such a way that it will follow the measured trajectory more precisely.

Data-Driven Algorithms: Theory and Applications

Virtual flow metering is fundamentally an extrapolation problem, namely with the set of measurements over a defined training period it is necessary to predict the future state of the system utilizing testing data. Data-driven forecasting algorithms can be distinguished between the statistical[12], such as regression and autoregression, or machine learning methods[13]. In this study, the virtual flow meter is built using various types of neural networks, which are outlined in this section.

The basic feedforward ANN is one of the most commonly used data-driven methods for prediction problems. It consists of interconnected neurons transferring information to each other and characterized by weights, biases, and nonlinear activation functions. Although it was superseded by complex deep learning methods, ANN is still frequently used as a baseline model for many forecasting tasks. The main disadvantage of ANN is that the information is only transferred from input to output, leading to poor performance in highly dynamic systems.

In contrast, the recurrent neural networks are more suitable to deal with transient data. Long short-term memory (LSTM) is a well-known example of a deep learning method and accounts both for short-term and long-term dynamics in the data[14]. The GRU in a way is similar to LSTM, but characterized by a simpler architecture with fewer parameters, and therefore, it is significantly faster to train using fewer hardware resources[15].

Ensemble learning methods is another class of techniques for prediction. The main idea behind this is to construct a combination of multiple learning algorithms that perform better than if used individually. Boosting is an efficient method for nonlinear forecasting that defines the predictor by combining many simple models. The example of a simple model, which is also referred to as the base model, can be a regression tree. Once these simple models are processed via a boosting algorithm, an accurate prediction can be made. Extreme gradient boosting (XGBoost) is a popular modern algorithm for oil and gas applications, which is more intuitive and flexible contrary to regular machine learning methods[16].

In this article, different data-driven methods are analyzed. ANN is chosen as a baseline method and compared to the performance of recurrent GRU and ensemble XGBoost. The evaluation is done on two use cases describing the prediction of multiphase rates in different production scenarios. It should be stressed that similar problems have been considered earlier[17], with different types of neural networks, such as LSTM and temporal convolutional networks.

Despite the variety of machine learning methods available, the workflow for preparation and practical deployment is similar. First, the time series of measurements, $X(t)$, together with the time series of target rates, $Y(t)$, are considered. Both are time-dependent, with the number of data points equal to the number of available measurements over some interval. The problem of the multiphase flow rate estimation can also be defined as time series regression following the machine learning nomenclature.

All of the data is split into two parts. The first part is needed to prepare (train) the model, and the second one is used to test the performance of the algorithm. Both parts of the data are first transformed into multiple sequences. Then, each component from X is mapped to a corresponding entry of Y. Normally, the length of each element of the input sequence equals several time steps, while the target sequence is presented by a single point only; therefore, measurements with history are used to predict the values of multiphase rates at a current time (sequence-to-point). The number of shifted time steps in the input sequence is one of the tuning parameters in the data-driven method, Fig. 2.

In summary, the data-driven virtual flow meter is a computational operator that relates X to the entries of vector Y.

$$X(t) \xrightarrow{VFM} Y(t). \quad (1)$$

This operator is initially obtained during the training phase and then used to make predictions of multiphase rates using the sequence-to-point prediction scheme.

Fig. 2 *The sequence-to-point prediction scheme.*

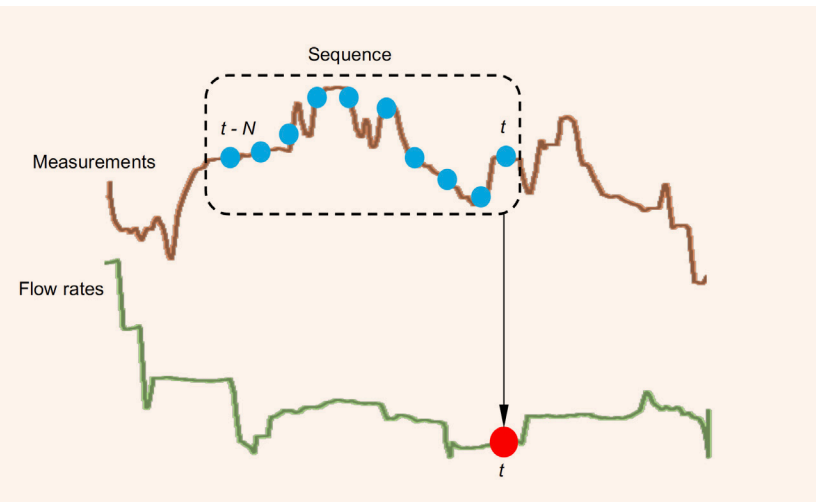

Practical Example 1: Simulated Production Data

A simplified example of a production system is considered in the first scenario, Fig. 3. The geometry of a well is defined by a horizontal part followed by a vertical segment of the well. The last part of the horizontal section is slightly inclined downwards to induce additional flow dynamics. The fluids from the reservoir enter the well via perforations located close to the inlet, which is simulated by individual source terms for liquid, gas, and water. Wellbore production is controlled using a topside choke.

Pressure and temperature sensors installed downhole provide continuous information about the wellbore's performance. Topside measurements for oil, gas, and water rates are provided by a generic multiphase flow. If the flow rate measurements become unavailable for some reason, the values of all flow rates need to be estimated using a concept of a data-driven virtual flow meter using only the readings from pressure and temperature gauges.

All the flow data was generated using the commercially available multiphase OLGA simulator[18]. The simulations have been performed for 4 hours of production, distinguished by three different production regimes defined by different choke settings. The total number of data points is 7,200 per one time series. The first half is used to setup the virtual flow meter via training of a machine learning algorithm, and the rest is used to utilize the quality of estimated values. The accuracy of predictions is evaluated using a normalized relative error, which defines the deviation of prediction over the true value within the full-scale range, Eqn. 2:

$$Normalized\ relative\ error = \frac{|Q_{PREDICTED} - Q_{TRUE}|}{Q_{TRUE\ MAX} - Q_{TRUE\ MIN}} \cdot 100\% \qquad 2$$

All three machine learning algorithms discussed in the previous section were used as candidates for the data-driven virtual flow meter. The architecture of all methods was chosen empirically to ensure convergence during training and good predictive capabilities. The ANN was built with three hidden layers, with 50 neurons for each layer. The structure of the deep GRU network was set up similarly with three hidden layers and 25 units in each layer. The XGboost architecture included 150 estimators and L1 regularization term equal to 0.1, with all other parameters set to default.

The length of the input sequences for ANN and GRU was set to 60 time steps, while for XGBoost it was set to 20 time steps only. The example of estimates with XGBoost is given in Fig. 4, where the predictions are plotted with red, the true values are depicted with blue, and the vertical dashed line indicates the split between the training and test data sets.

The accuracy of predictions defined by Eqn. 2 is slightly decreased for the test data, while it is still reasonably good for most of the time data. The error might exhibit instantaneous values up to 35% during a rapid increase of the observed flow rates, though on average it is well within the acceptable range — below 5% relative. This is indicated in Fig. 5 where the uncertainty distribution for all three prediction methods used is plotted.

The performance of all predictive methods is compared in Table 1, where the integrated characteristics of each model are given. The error distribution is averaged over the entire testing period for each time series predicted and then averaged again over all three fluid phases. The training time corresponds to the computational effort, which is required to prepare a model on a regular desktop computer. As it follows from the obtained results, the GRU network produced the most accurate results,

Fig. 3 *A schematic description of the production system for the virtual flow meter application.*

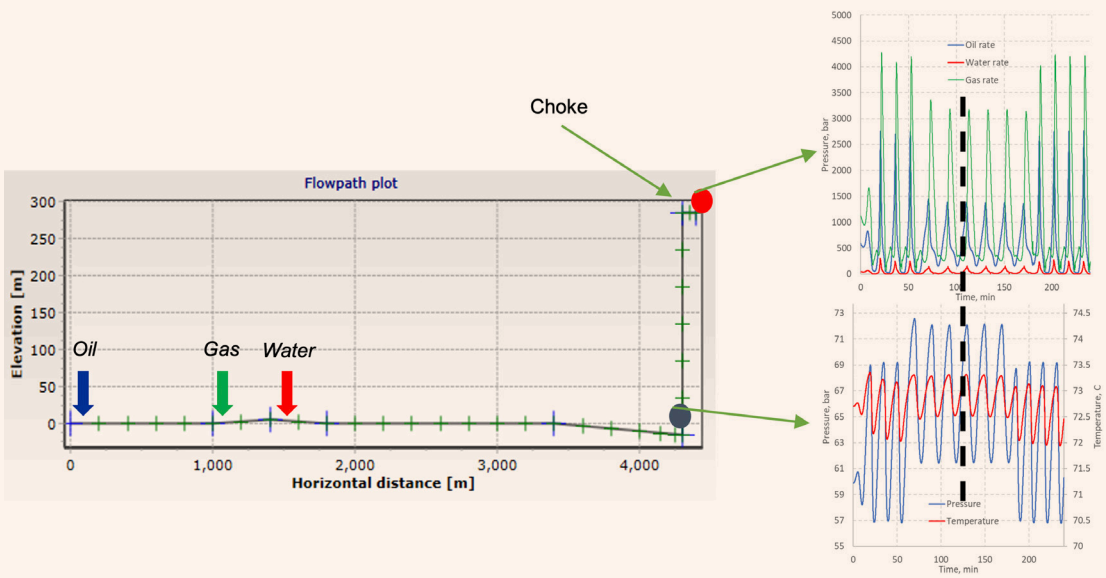

Fig. 4 *An example of the estimated multiphase rates of (a) gas, (b) oil, and (c) water (from left to right) with XGBoost. The dashed vertical line divides the training and test data sets.*

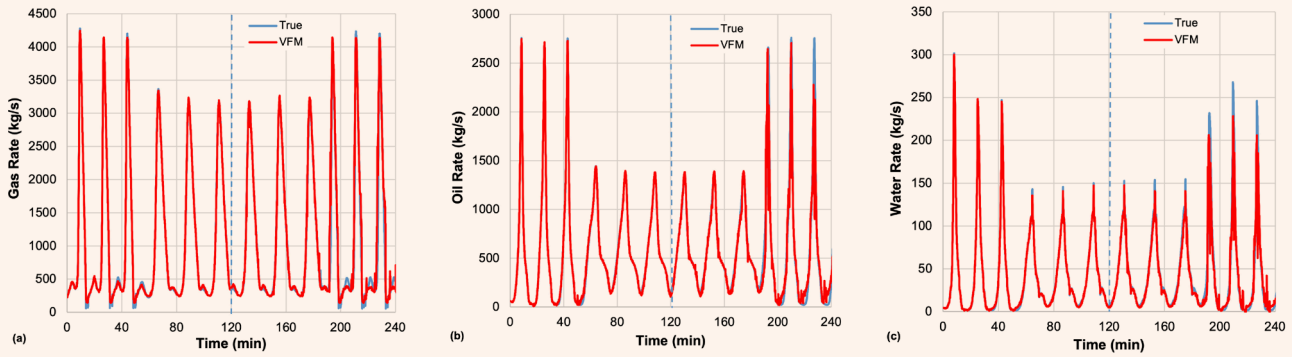

Fig. 5 *Relative uncertainty (a) gas, (b) oil, and (c) water predictions with different methods. The dashed vertical line divides the training and test data sets.*

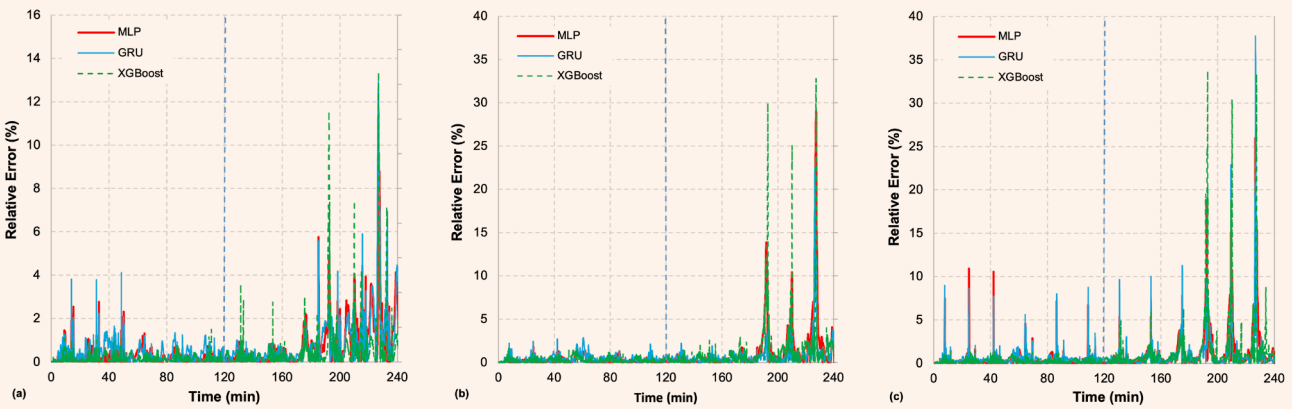

Table 1 *Comparing the performance of data-driven methods.*

	Average Error (%)	Training Time (s)
ANN	1.37	294
GRU	1.25	1,690
XGBoost	2.63	1.08

however, the required time for its training was significant.

The accuracy of the ANN is comparable to the GRU, although the model was trained approximately five times faster. With the XGBoost, which produced the least accurate results, the model was trained almost instantly. It is noted that the accuracy of the last method could be improved by choosing the best possible hyperparameters using a cross validation technique. Subsequently, even with the obtained accuracy, XGBoost can be considered as a computationally efficient tool to perform an initial screening of the available data. The use of advanced methods such as GRU is not justified, as it does the same job as a regular neural network, but requires more time.

Practical Example 2: Simulated Well Test Data

Another practical example considers a publicly available data set discussing transient well testing. This data set has already been analyzed from the point of virtual flow metering[17, 19]. The data set includes the simulated time series of input pressure and temperature measurements and output flow rates, which are represented by five different time intervals. Each interval corresponds to a certain choke opening, leading to different behavior in the data, which varies from almost static (first and the last periods) to fully dynamical. The measurements are also corrupted by the noise, which complicates the analysis, Figs. 6 and 7.

The prediction scheme is formulated similarly to the previously discussed problem: given pressure and temperature measurements as inputs, it is necessary to forecast the multiphase flow rates of oil, gas, and water. The

Fig. 6 The pressure and temperature measurements (inputs).

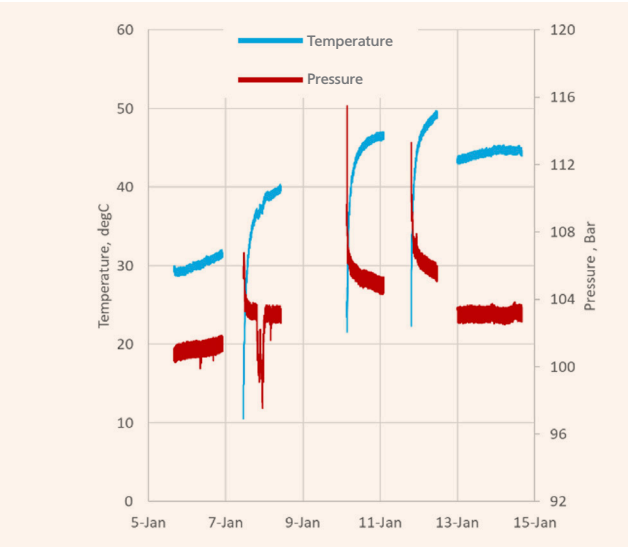

Fig. 7 The flow rate time series (outputs).

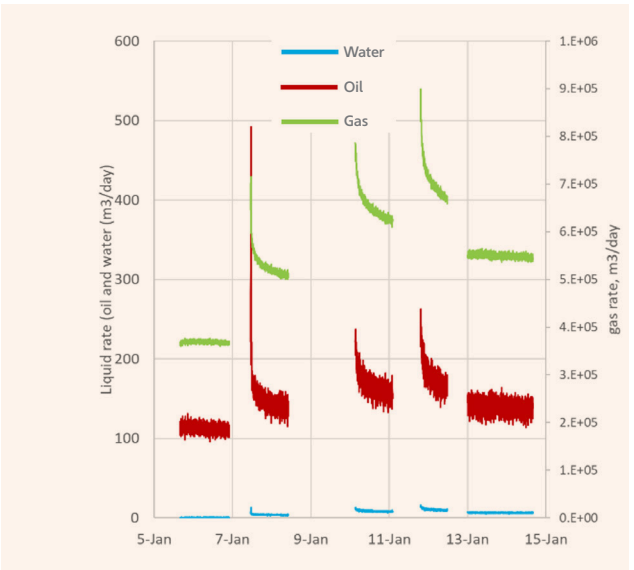

machine learning model was first prepared by splitting all the available data for training and testing, which includes the first three and last two flow intervals, respectively. Second, the data was preprocessed: the noisy component was removed by the Savitzky-Golay filter[20]. This filter approximates the time series data by a finite number of low degree polynomials, which ensures minimal loss of information, compared to other methods such as the low pass filter or moving average. Before the actual training, the feature scaling was used, which effectively centered the data around the mean with a unit standard deviation.

For all three methods (ANN, GRU, and XGBoost), the data was split into sequences of 10 time steps each for training and prediction purposes. Both the ANN and GRU employed a similar architecture, where three hidden layers with 10 neurons were used. XGboost was set up with 500 estimators and *L1* regularization term equal to 0.9, and *L2* regularization term equal to 10, with default values for all remaining parameters. The evaluation of all three models for both training and test data sets is given in Figs. 8 to 10, where the estimated flow rates are depicted by the black curve compared to the noisy ground truth.

The simulated results are summarized in Table 2. For the accuracy, the average relative error over the whole testing data is compared.

Based on the results, the general performance of the ANN is the best among the methods used. Subsequently, looking at the quality of predictions one could notice that a regular neural network is unable to reconstruct properly complex nonlinearities in the data. This is illustrated at best by the second flow period in the training data set, where the ANN follows a non-monotonic behavior, which is transferred to the solution from the input pressure time series.

Both the GRU and XGBoost, in contrast, better describe the data and do better prediction despite the average quality metric being worse. Despite the conclusion for the previous case, for that particular scenario, the application of a recurrent network is well advised. Moreover, the best results have been obtained with XGBoost, which demonstrated the best quality results at the shortest training time.

Conclusions

The application of different data-driven methods for the problem of production time series analysis and forecasting has been analyzed in this work. Following the results of computationally based scenarios, the suggested open loop approach for the virtual flow metering is a convenient and robust tool to make forecasts directly from the data. This work can be summarized as follows:

- Different approaches for virtual flow metering have been considered, outlining the importance of flow modeling, which is a core component of any methods for intelligent production monitoring.
- Various data-driven algorithms are introduced and evaluated for the practical applications of production data forecasting.
- Depending on the use case considered, different types of machine learning methods could have advantages over each other. Generally, the choice of more advanced techniques is reasonable, although the computational effort to prepare the model is increased.
- In most cases the use of a regular ANN or advanced XGBoost is sufficient to provide baseline estimates for most types of production data available.

The future work should be concentrated around the practical application for real-life scenarios. The problem of measurement noise, which was simply filtered out in this application, would require special treatment, especially for any measurement outside the training range.

Fig. 8 *The multiphase rates forecast for the ANN trained on the first three flow periods: (a) oil, (b) water, and (c) gas rates.*

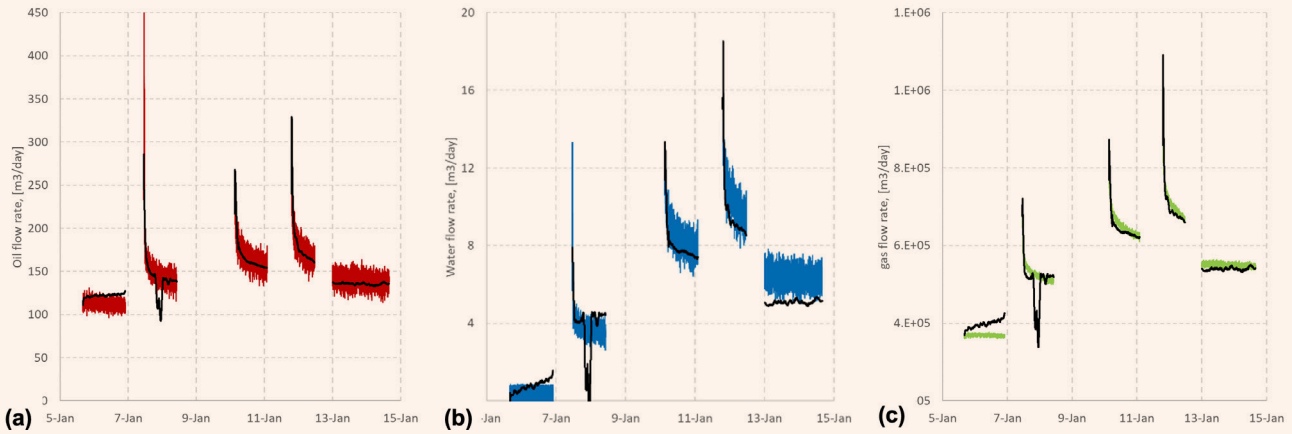

Fig. 9 *The multiphase rates forecast for the GRU trained on the first three flow periods: (a) oil, (b) water, and (c) gas rates.*

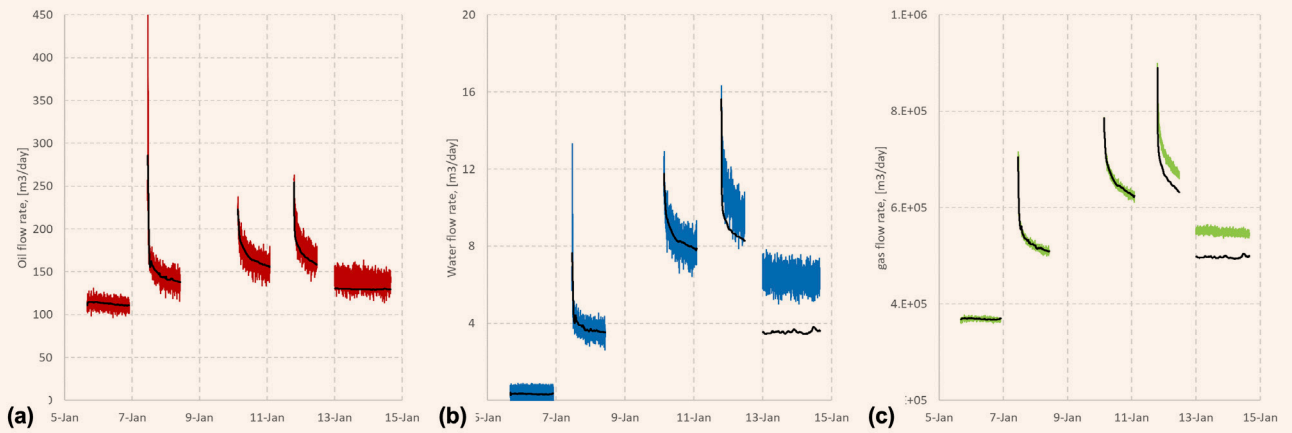

Fig. 10 *The multiphase rates forecast for the XGBoost trained on the first three flow periods: (a) oil, (b) water, and (c) gas rates.*

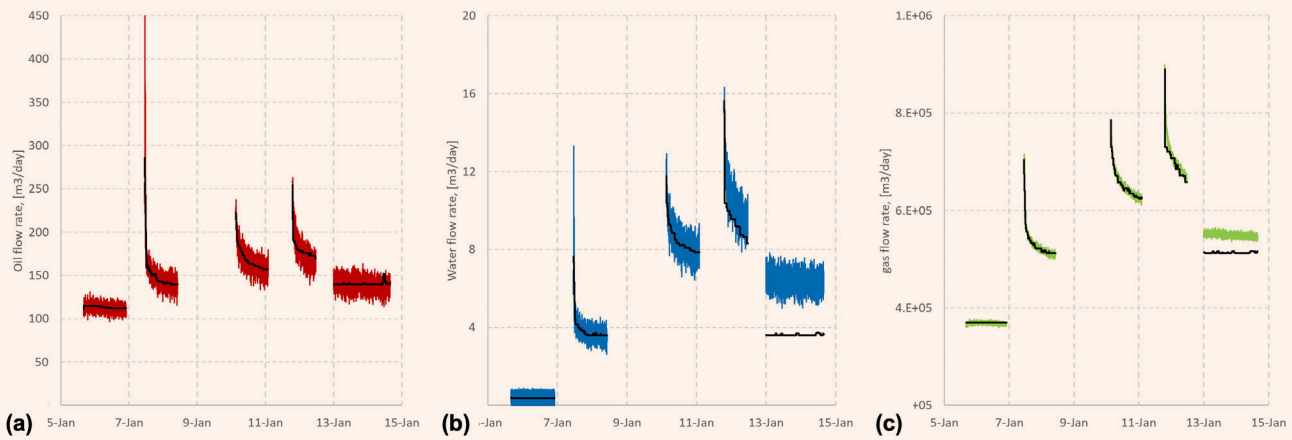

Table 2 *The simulated test data results for the three methods.*

	Accuracy (%)			Training Time (s)
	Oil	**Water**	**Gas**	
ANN	4.8	14.5	1.97	33
GRU	5.87	26.7	6.2	149
XGBoost	4.51	25.37	3.68	0.94

Acknowledgments

This article was prepared for presentation at the SPE Symposium: Artificial Intelligence — Toward a Resilient and Efficient Energy Industry, al-Khobar, Saudi Arabia, October 18-19, 2021.

References

1. Bikmukhametov, T. and Jäschke, J.: "First Principles and Machine Learning Virtual Flow Metering: A Literature Review," *Journal of Petroleum Science and Engineering*, Vol. 184, January 2020.
2. Spesivtsev, P., Sinkov, K., Sofronov, I., Zimina, A., et al.: "Predictive Model for Bottom-hole Pressure Based on Machine Learning," *Journal of Petroleum Science and Engineering*, Vol. 166, July 2018, pp. 825-841.
3. Omrani, P.S., Dobrovolschi, I., Belfroid, S., Kronberger, P., et al.: "Improving the Accuracy of Virtual Flow Metering and Back Allocation through Machine Learning," SPE paper 192819, presented at the Abu Dhabi International Petroleum Exhibition and Conference, Abu Dhabi, UAE, November 12-15, 2018.
4. Gryzlov, A., Safonov, S., AlKhalaf, M. and Arsalan, M.: "Novel Methods for Production Data Forecast Utilizing Machine Learning and Dynamic Mode Decomposition," SPE paper 202792, presented at the Abu Dhabi International Petroleum Exhibition and Conference, Abu Dhabi, UAE, November 9-12, 2020.
5. Spesivtsev, P.E., Kharlashkin, A.D. and Sinkov, K.F.: "Study of the Transient Terrain-Induced and Severe Slugging Problems by Use of the Drift-Flux Model," *SPE Journal*, Vol. 22, Issue 5, October 2017, pp. 1570-1584.
6. Kanin, E.A., Osiptsov, A.A., Vainshtein, A.L. and Burnaev, E.V.: "A Predictive Model for Steady-State Multiphase Pipe Flow: Machine Learning on Lab Data," *Journal of Petroleum Science and Engineering*, Vol. 180, September 2019, pp. 727-746.
7. Robertson, D.G. and Lee, J.H.: "A Least Squares Formulation for State Estimation," *Journal of Process Control*, Vol. 5, Issue 4, August 1995, pp. 291-299.
8. Jazwinski, A.H.: *Stochastic Processes and Filtering Theory*, 1st edition, Academic Press, New York, 1970, 376 p.
9. Gryzlov, A., Safonov, S., AlKhalaf, M. and Arsalan, M.: "Dynamic Mode Decomposition for Virtual Flow Metering," *EAGE Geomodel 2020*, Vol. 2020, September 2020, pp. 1-5.
10. Lorentzen, R.J., Stordal, A.S., Luo, X. and Naevdal, G.: "Estimation of Production Rates by Use of Transient Well Flow Modeling and the Auxiliary Particle Filter: Full-Scale Applications," *SPE Production and Operations*, Vol. 31, Issue 2, May 2016, pp. 163-175.
11. Gryzlov, A., Mudde, R.F. and Schiferli, W.: "Inverse Modeling of the Inflow Distribution for the Liquid/Gas Flow in Horizontal Pipelines," paper presented at the 14th International Conference on Multiphase Production Technology, Cannes, France, June 17-19, 2009.
12. Ho, S.L. and Xie, M.: "The Use of ARIMA Models for Reliability Forecasting and Analysis," *Computers and Industrial Engineering*, Vol. 35, Issues 1-2, October 1998, pp. 213-216.
13. Sagheer, A. and Kotb, M.: "Time Series Forecasting of Petroleum Production Using Deep LSTM Recurrent Networks," *Neurocomputing*, Vol. 323, January 2019, pp. 203-213.
14. Hochreiter, S. and Schmidhuber, J.: "Long Short-Term Memory," *Neural Computation*, Vol. 9, Issue 8, November 1997, pp. 1735-1780.
15. Cho, K., van Merrienboer, B., Gulcehre, C., Bahdanau, D., et al.: "Learning Phrase Representations Using RNN Encoder-Decoder for Statistical Machine Translation," paper published in *Proceedings of the 2014 Conference on Empirical Methods in Natural Language Processing (EMNLP)*, October 2014, pp. 1724-1734.
16. Chen, T. and Guestrin, C.: "XGBoost: A Scalable Tree Boosting System," paper published in *Proceedings of the 22nd ACM SIGKDD International Conference on Knowledge Discovery and Data Mining*, August 2016, pp. 785-794.
17. Gryzlov, A., Mironova, L., Safonov, S. and Arsalan, M.: "Artificial Intelligence and Data Analytics for Virtual Flow Metering," SPE paper 204662, prepared for presentation at the SPE Middle East Oil and Gas Show and Conference, Manama, Kingdom of Bahrain, November 28-December 1, 2021.
18. Bendiksen, K.H., Maines, D., Moe, R. and Nuland, S.: "The Dynamic Two-Fluid Model OLGA: Theory and Application," *SPE Production Engineering*, Vol. 6, Issue 2, May 1991, pp. 171-180.
19. Andrianov, N.: "A Machine Learning Approach for Virtual Flow Metering and Forecasting," paper presented at the 3rd IFAC Workshop on Automatic Control in Offshore Oil and Gas Production, Esbjerg, Denmark, May 30-June 1, 2018.
20. Savitzky, A. and Golay, M.J.E.: "Smoothing and Differentiation of Data by Simplified Least Squares Procedures," *Analytical Chemistry*, Vol. 36, Issue 8, July 1964, pp. 1627-1639.

About the Authors

Dr. Anton Gryzlov

Ph.D. in Applied Physics, Delft University of Technology

Dr. Anton Gryzlov is a Petroleum Engineering Specialist working at the Aramco Innovations Global Research Center (GRC) in Moscow, Russia. He is involved in the development of intelligent solutions for multiphase flow metering and optimization and control.

Prior to joining the newly established Moscow GRC in 2019, Anton worked for 14 years in various positions related to different aspects of multiphase flow metering development and commercialization. This includes extensive R&D experience at Roxar and Schlumberger.

He is the author of more than 15 technical publications on fluid flow, including Society of Petroleum Engineering (SPE) proceedings and papers in peer-reviewed journals.

In 2005, Anton received his M.S. degree in Mechanical Engineering from Bauman Moscow State Technical University, Moscow, Russia. In 2010, he received his Ph.D. degree in Applied Physics from Delft University of Technology, Delft, the Netherlands.

Liliya Mironova

M.S. in Information Systems and Technologies, Skolkovo Institute of Science and Technology

Liliya Mironova is a Data Scientist working at the Aramco Innovations Global Research Center in Moscow. Her technical expertise is with applying traditional machine learning and deep learning methods for time-series prediction and analysis.

Prior to joining the Moscow Research Center, she was a Software Development Engineer at Intel.

Liliya received her B.S. degree in Computer Science from the Moscow Institute of Physics and Technology, and her M.S. degree in Information Systems and Technologies from the Skolkovo Institute of Science and Technology, Moscow, Russia.

Dr. Sergey Safonov

Ph.D. in Quantum Semiconductor Physics, University of Exeter

Dr. Sergey Safonov is a Research Program Director working at the Aramco Innovations Global Research Center in Moscow, Russia. He is currently leading a new team of research data scientists focusing on developing new digital solutions using novel artificial intelligence, machine learning, and data analytics technologies.

Sergey has 15 years of R&D experience in upstream oil and gas gained from working on various research positions in Schlumberger in Russia and in the U.K. He has extensive experience in multidomain aspects of multiphase fluid flow, advanced core analysis, digital rock modeling, and drilling processes.

Sergey is the author of more than 30 scientific and technical papers, including Society of Petroleum Engineering (SPE) proceedings and papers in peer-reviewed journals.

He received his M.S. degree in Applied Physics from the Moscow Institute of Physics and Technology, Moscow, Russia, and his Ph.D. degree in Quantum Semiconductor Physics from the University of Exeter, Exeter, U.K.

Dr. Muhammad Arsalan

Ph.D. in Electronics Engineering, Carleton University

Dr. Muhammad Arsalan joined Saudi Aramco in 2013 as a Senior Research Scientist. He is leading a team of experts in multiphase metering, sensing, intervention, and robotics focus area within the Production Technology Division of Saudi Aramco's Exploration and Petroleum Engineering Center – Advanced Research Center (EXPEC ARC). Muhammad is also leading the global digital transformation team of EXPEC ARC in advanced sensing domain. His team is working on innovative surface and subsurface production monitoring, control, and optimization technologies.

Muhammad is a seasoned professional with over 20 years of experience in academia and various industries, including biomedical, space, chemicals, and oil and gas. He has over 100 international granted patents and publications related to integrated sensors, systems, and tools.

Muhammad is the recipient of several major national and international awards and distinctions for his entrepreneurial skills and his groundbreaking contributions to the innovation, research and technology development.

Muhammad is the co-founder of two North American technology startups.

In 2004, he was an Invited Researcher and Natural Sciences and Engineering Research Council–Japan Society for the Promotion of Science (NSERC–JSPS) Fellow with the Tokyo Institute of Technology. From 2005 to 2008, Muhammad was an NSERC Alexander Graham Bell Graduate Scholar with the Carleton University.

From 2009 to 2010, he was a National Aeronautics and Space Administration (NASA) postdoctoral Fellow. In 2010, Muhammad joined King Abdullah University of Science and Technology (KAUST) in Thuwal, Saudi Arabia, as an NSERC postdoctoral Research Fellow.

From 2011 to 2016 he was an Adjunct Research Professor with Carleton University, Ottawa, Canada.

Muhammad received his B.Eng. degree from the Institute of Industrial Electronic Engineering, NED University of Engineering and Technology, Karachi, Pakistan in 1999, and his M.S. and Ph.D. degrees, both in Electronic Engineering, from Carleton University, Ottawa, Ontario, Canada, in 2004 and 2009, respectively.

SmartWater Synergy with Microsphere Injection for Permeable Carbonates

Dongqing Cao, Dr. Ming Han, Salah H. Saleh, Dr. Subhash C. Ayirala and Dr. Ali A. Yousef

Abstract /

This article presents a laboratory study on the combination of SmartWater with microsphere injection to improve oil production in carbonates, which increases the sweep efficiency and oil displacement efficiency. In this study, the properties of a micro-sized polymeric microsphere were investigated, including size distribution, rheology, and zeta potential in SmartWater, compared with conventional high salinity water (HSW). Coreflooding tests using natural permeable carbonate cores were performed to evaluate flow performance and oil production potential at 95 °C and 3,100 psi pore pressure. The flow performance was evaluated by the injection of 1 pore volume (PV) microspheres, followed by excessive water injection. Oil displacement tests were also performed by injecting 1 PV of microspheres dissolved in SmartWater after conventional waterflooding.

The median particle size of the microsphere in conventional injection water with a salinity of 57,670 ppm was about 0.25 μm. The particle size was increased by 50% to 100% with reduced elastic modulus when the microsphere was dispersed in SmartWater with lower salinity. The zeta potential value of the microsphere was decreased in SmartWater compared to that in the conventional injection water, showing a more negatively charged property. The flow performance of microsphere solutions in the carbonate cores was found to be dependent on their particle size, strength, and suspension stability.

The results from the coreflooding tests showed that the microsphere dispersed in SmartWater would result in higher differential pressure than that observed in conventional injection water. The SmartWater caused the microspheres to swell larger, but with softer particles and with better suspension stability, which enhanced both the migration and blocking efficiency of the microsphere injection. The oil displacement tests confirmed that the microsphere in SmartWater displaced more oil than that obtained with conventional injection water.

This result was clearly supported by the higher differential pressure from the microsphere injection in SmartWater. The oil bank appeared hysteretically in the post-water injection stage, which was quite different from the reported findings of typical mobility controlling agents in the existing knowledge. The microspheres were observed in the coreflood produced fluids, indicating the improvement of microsphere migration by SmartWater.

This work, for the first time, demonstrates that the combination of SmartWater and microsphere injection yields additional oil production. The proposed hybrid technique can provide a cost-effective way to improve waterflooding performance in heterogeneous carbonates.

Introduction

SmartWater, by tuning ion compositions of injection water, is a technology to increase oil production in carbonate reservoirs[1,2]. The mechanisms of effective oil displacement by SmartWater in carbonates were reported as wettability alteration[3-5], multicomponent ion exchange[6,7], mineral dissolution[8], fines migration[9], and pH increase[7,10]. Besides these mechanisms focusing on fluid-rock interface, SmartWater positively impacted released oil ganglion dynamics for efficient oil mobilization through the interactions at the fluid-fluid interface[11-13]. A single well chemical tracer test demonstrated the promising potential of SmartWater with approximately seven saturation unit reductions in residual oil after conventional water injection in permeable carbonate[14].

SmartWater injection with other chemicals is considered as a potential optimization route to improve the performance by enhancing or supplementing the displacement mechanisms. The chemical flooding agents, such as polymer, surfactant, and alkaline, showed good synergy effects and positive oil displacement results with SmartWater[15-17]. Researchers have also studied the performance of low salinity water combined with several gel materials, such as preformed particle gels (PPG) and bulk gels in the fractured reservoir. Alhuraishawy et al. (2016, 2017)[18,19] combined low salinity water flooding and PPG to increase oil production in fractured carbonate reservoirs.

Compared to traditional bulk gel treatments, PPG formed stronger plugging but did not form an impermeable cake in the fracture surface; therefore, PPG allowed low salinity water to penetrate into the matrix to modify its wettability, thereby producing more oil from the matrix. Alhuraishawy et al. (2017)[20] also studied the combined

low salinity and PPG in various fractured core models, including a five-spot sandstone model, a non-crossflow heterogeneous model[21], open fractures, and partially open fractures[19, 20, 22]. Brattekas et al. (2015, 2020)[23, 24] studied the low salinity chase waterflooding after bulk gel placement. The results showed that low salinity water improved the blocking capacity of the gel, and subsequently flooded the matrix during chase floods, which provided additional benefits to the waterflooding.

Microsphere, a kind of particle gel, has drawn great attention due to the unique properties for in-depth fluid diversion in permeable sandstone and carbonate in recent years[25-27]. Synthesized by the inverse emulsion polymerization method[28], the polymeric microsphere presents a uniform spherical shape. With a crosslinking structure, the thermal and mechanical stabilities are better than the corresponding linear polymer[29, 30]. Similar with other gel materials, the microsphere has complementary mechanisms on oil production with SmartWater.

The mechanism of microsphere injection is to sterically block the flow channel by adsorption or strain and divert the flow to the uninvaded areas and increase the sweep efficiency. The particle size of the microsphere ranges from a nanometer to a micron, which is in the same level with the pore size of the permeable reservoir. This makes the microsphere applicable to the reservoir matrix, which is different from PPG or bulk gel. Compared with water-soluble chemicals, microsphere is a chemically stable material, it has no negative effect on the low salinity water/rock/crude oil interactions. SmartWater can work normally and produce more oil in the unswept area. SmartWater synergy with microsphere injection can be a novel hybrid technique to increase the sweep efficiency and oil displacement efficiency in permeable carbonate reservoirs.

In this work, the effect of SmartWater on the microsphere bulk properties was evaluated. The flow properties and oil production performance of SmartWater synergy with microsphere injection were investigated by using coreflooding tests.

Experimental

Brine and Chemicals

Synthetic injection water and SmartWater were used to prepare the microsphere solutions. The total dissolved salt (TDS) of the high salinity water (HSW) as injection water was 57,670 mg/L. SmartWater is a kind of low salinity water with optimized ion composition. In this work, the 10 times and 100 times diluted injection water were tentatively used as SmartWater for evaluation purpose. Connate water was used to saturate the core plugs. Table 1 shows the ion compositions of the brines. The crude oil was degassed oil with viscosity of 2 mPa.s at 95 °C.

Microsphere

The microsphere was initially in the form of W/O emulsion. The microsphere was in the water phase with a solid content of 39.5%. The microsphere sample was prepared in volume percentage. The method was to add quantitative microsphere into the brines by magnetically stirring them at 800 rpm.

Microsphere Bulk Property Test

The bulk properties of the microsphere in brines, including particle size, zeta potential, and strength were tested. The particle size of the microsphere samples was measured by using a laser diffraction particle size analyzer. The zeta potential of the microsphere was tested by a Malvern zeta potential analyzer. The strength of the concentrated microsphere samples was measured by the strain sweep and frequency sweep using a TA Instruments rheometer.

Table 1 *The ion compositions of the brines used.*

Ion	Na^+ (mg/L)	Ca^{2+} (mg/L)	Mg^{2+} (mg/L)	Cl^- (mg/L)	HCO_3^- (mg/L)	SO_4^{2-} (mg/L)	TDS (mg/L)
HSW	18,300	650	2,110	32,200	120	4,290	57,670
SmartWater 1	1,830	65	211	3,220	12	429	5,767
SmartWater 2	183	6.5	21.1	322	1.2	42.9	576.7
Connate Water	59,491	19,040	2,439	132,060	354	350	213,734

Table 2 *Basic information of the carbonate core plugs used in the test.*

Core No.	Diameter (cm)	Length (cm)	PV (ml)	Brine Perm. (mD)	Original Oil in Core (ml)	Test Type
31	3.83	4.13	12.838	405	—	Microsphere injection test
241	3.80	3.85	8.713	460	6.852	Oil displacement test
44	3.81	4.24	10.071	420	9.181	Oil displacement test

Fig. 1 *Diagram sketch of the coreflooding system.*

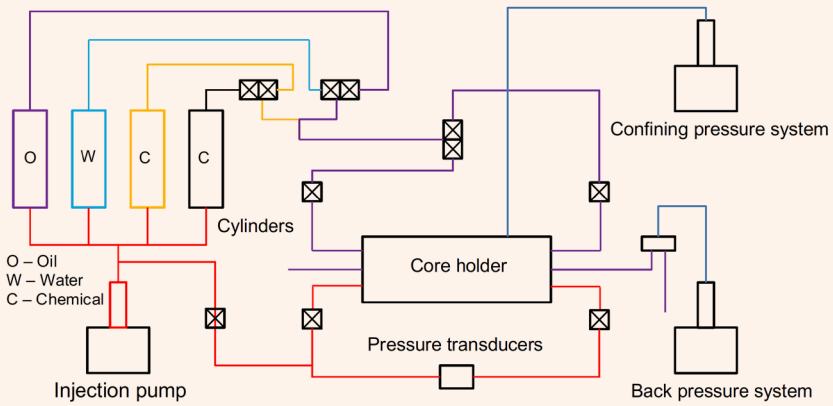

Core Plugs

The core plugs in the microsphere injection tests and oil displacement tests were natural carbonate cores. Table 2 shows the basic core information and usage in the tests. The permeability of the three core plugs was from 405 mD to 460 mD, which were typical permeable carbonates.

Microsphere Injection Test

The microsphere injection tests were conducted by the AFS-300 coreflooding system, Core Lab, USA. Figure 1 is a diagram sketch of the system. The procedures are as follows:

1. Saturate the core plug with connate water by vacuum.
2. Load the core plug into the core holder. Set the confining pressure at 600 psi and the pore pressure at 100 psi.
3. Test the brine permeability of the core by connate water at different flow rates of 0.5 cc/min, 1 cc/min, and 2 cc/min.
4. Flush the core plug with injection water for 5 pore volumes (PV).
5. Heat the core holder to 95 °C and balance for 4 hours. Increase the confining pressure and pore pressure step by step to 4,500 psi and 3100 psi, respectively.
6. Test the baseline pressure by injection water at 0.5 cc/min.
7. Inject the microsphere solution at 0.5 cc/min and record the differential pressure.
8. Switch the flow to SmartWater at 0.5 cc/min for about 5 PV and record the differential pressure.
9. Perform additional injection water and SmartWater injection until a stable differential pressure is reached.

Oil Displacement Test

The performance of the microsphere on incremental oil production was evaluated by the oil displacement tests. The procedures are as follows:

1. Saturate the core plug with connate water by vacuum.
2. Load the core plug into the core holder. Set the confining pressure at 600 psi and the pore pressure at 100 psi.
3. Test the brine permeability of the core by connate water at different flow rates of 0.5 cc/min, 1 cc/min, and 2 cc/min. Unload the core plug from the core holder.
4. Saturate the core plugs with crude oil by high speed centrifuge at 6,000 r/min for 1 hour. Reverse the core plug and centrifuge again with the same rotational rate and time. Record the weight before and after centrifuge.
5. Age the saturated core at 95 °C for 3 weeks to restore the wettability.
6. Fresh oil flood. Reload the aged core into the core holder. Set the confining pressure to 600 psi and the back pressure to 100 psi. Inject fresh oil into the core to displace the aged oil.
7. Heat the core holder to 95 °C and balance for 4 hours. Increase the confining pressure and pore pressure step by step to 4,500 psi and 3,100 psi, respectively.
8. HSW flooding at 0.5 cc/min until a stable differential pressure and oil production. Perform a bump water flooding using flow rates of 1 cc/min, 2 cc/min, and 4 cc/min.
9. Microsphere in SmartWater injection at 0.5 cc/min for 1 PV.
10. Chase the HSW injection at 0.5 cc/min until a stable differential pressure and oil production is reached.

Results and Discussion

Microsphere Bulk Properties

The effect of SmartWater on the microsphere bulk properties was tested, including particle size, zeta potential, and strength. Figure 2 shows the particle size distribution of the microsphere in different brines. Table 3 summarizes

the microsphere's bulk properties in different brines. The microsphere is a macro solid particle in nature. When dispersed in the brines, the microsphere samples were homogeneous, white, and opaque liquid. The median particle size in the injection water was 0.25 μm. In the two kinds of SmartWater, the particle size increased to 0.32 μm and 0.67 μm.

The microsphere is a water swollen polymeric material. It has a macromolecular network that can contain a large fraction of water within their structure. This water absorbing capacity comes from the osmotic pressure between the brine and the microsphere network that drives the water into the polymeric network. Low salinity water increases the osmotic pressure between the microsphere and the brine and more water can be adsorbed into the microsphere. The swelling capacity is therefore improved.

Consequently, the strength of the particle decreased from 1,963 Pa to 1,678 Pa, due to absorbing water. The microsphere in brines is an unstable polydisperse system.

Fig. 2 *The particle size distribution of the microsphere in different brines.*

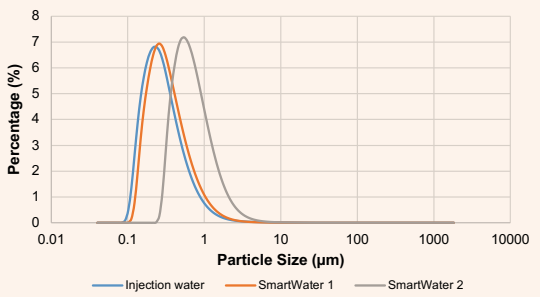

The particles tend to coalescent and precipitant, especially in the high salinity brines. Zeta potential is a key indicator of the coalescence and sedimentary stability of particle dispersions. As shown in Table 3, the zeta potentials of the microsphere sample in the injection water was very low as -4.5 mV. The high salinity compacted the electronic double layers of the colloid particle, resulting in the low zeta potential. In the two SmartWater samples, the zeta potential increased to -9.0 mV and -20.1 mV. The high zeta potential could improve the suspension stability of the microsphere samples.

Microsphere Flow Tests

Three microsphere flow tests were conducted to study the effect of SmartWater on the microsphere flow in the brine saturated carbonate cores. Table 4 shows the injection scenarios in the tests. The additional injection water and SmartWater injection after the first SmartWater injection was to check the pressure response of the retention microsphere in the core with salinity. SmartWater 2 with a much lower salinity was used in three tests to obtain comparative results.

Figures 3, 4, and 5 show the differential pressure change during the injection process in the three tests, respectively. In all three tests, the microsphere injection increased the differential pressure due to the steric blocking in the pores. For Test 1, in which the microsphere was suspended in SmartWater, the differential pressure increased from 0.05 psi to 0.24 psi during the 1 PV microsphere injection. The following SmartWater injection did not produce pressure change. An additional injection water and SmartWater injection was performed after the above two steps. As previously shown in Fig. 3, the differential pressure dropped abruptly when the injection switched to the HSW. When switch back to SmartWater, the differential pressure increased slowly back to a value close to the initial value.

In Test 2, the microsphere was dispersed in the injection

Table 3 *The microsphere's bulk properties in different brines.*

	Injection Water	SmartWater 1	SmartWater 2
Media Particle Size (μm)	0.25	0.32	0.67
Strength (Pa)	1,963	1,754	1,678
Zeta Potential (mV)	-4.5	-9.0	-20.1

Table 4 *Injection scenarios in microsphere flow tests.*

Test No.	Injection Scenarios
1	Microsphere in SmartWater (1 PV) → SmartWater → Injection water → SmartWater
2	Microsphere in injection water (1 PV) → SmartWater → Injection water → SmartWater
3	Microsphere in injection water (2 PV) → SmartWater → Injection water → SmartWater

Fig. 3 *The differential pressure in Test 1.*

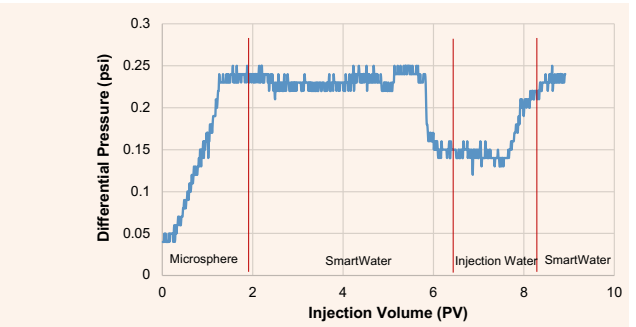

Fig. 4 *The differential pressure in Test 2.*

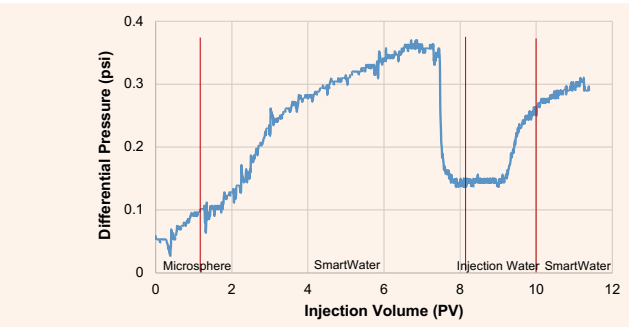

Fig. 5 *The differential pressure in Test 3.*

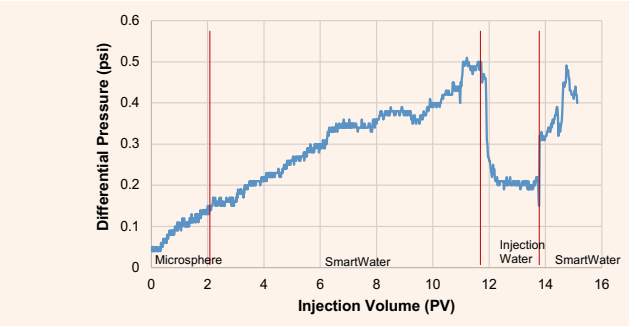

water. The differential pressure was increased to 0.1 psi after the 1 PV microsphere injection. Different from Test 1, the differential pressure kept increasing in the subsequent SmartWater injection until a relative stable value was reached. In the additional injection water and SmartWater injection, the differential pressure behaved similar as in Test 1.

Test 3 used the same injection scenarios but a larger microsphere injection volume compared with Test 2. Consequently, the differential pressure was higher than Test 2.

The swelling capacity and dispersion stability of the microsphere with the brine salinity could be the reason of the differences. The microsphere in SmartWater had a larger particle size than in the injection water. This made the microsphere easily strain and block the pores. Therefore, the differential pressure produced by microsphere injection in Test 1 was higher than in Test 2. In the following SmartWater injection, the microsphere could swell in Test 2 because it was initially dispersed in the injection water. This resulted in the continuous pressure increase in Test 2. The maximum differential pressure was even higher than Test 1.

The swelling of the microsphere in SmartWater seems to be reversible. In the additional injection water and SmartWater injection, the differential pressure decreased or increased with the switch of water salinity. This could be used as a potential way to improve the microsphere deep migration capacity. Another impact of SmartWater on the microsphere is the suspension stability. The microsphere suspension tends to coalesce to large aggregates, especially at high temperature and high salinity conditions.

When injected into the cores, the particles could be stuck due to the size exclusion to the large aggregates. This could happen in the test that the microsphere was suspended in the HSW. Microsphere particles are charged on the surface due to the hydrolysis of the polar group in the brine. SmartWater can increase the zeta potential of the microsphere and make the particle more repellent. The suspension stability is therefore enhanced, and less aggregates were formed with a better migration capacity; however, the improved particle size seems the dominate factor in this case.

Oil Displacement Tests

Two oil displacement tests were performed on carbonate core plugs to evaluate the oil production performance of the microsphere in SmartWater after the water injection. HSW was used in the waterflooding. To eliminate capillary end effect, a bump HSW flooding was performed using flow rates of 1 cc/min, 2 cc/min, and 4 cc/min at the end of the waterflooding. The microsphere was suspended in SmartWater instead of injection water. The two tests used SmartWater 1 and SmartWater 2, respectively, as listed in Table 5 to study the effect of the salinity. The last step was to chase the HSW injection to evaluate if there was any positive response during the salinity variation.

The oil production and differential pressure of the two tests — Test 4 and 5 — are shown in Figs. 6 and 7, respectively. Test 4 used the microsphere in SmartWater 1, and the HSW injection produced oil of 27.7%. The three bump floods totally increased oil production by 11.7%, indicating severe end effect. At each flow rate, the differential pressure first burst up and then decreased to stable. After the bump floods, the flow rate resumed 0.5 cc/min until a stable differential pressure. The following microsphere injection increased differential pressure from 0.08 psi to 0.48 psi. Almost no oil was produced during the 1 PV microsphere injection. The oil bank appeared in the post-HSW injection. The oil production

Table 5 *The microsphere and core plugs used in the oil displacement tests.*

Test No.	Fluid	Core Plug
4	0.5% Microsphere suspended SmartWater 1	241
5	0.5% Microsphere suspended SmartWater 2	44

increased by 3.9% at the end of the post-water injection.

Test 5 used the microsphere in SmartWater 2, and the oil production of waterflooding at 0.5 cc/min was 33.2%. The three bump floods totally increased oil production by 12.5%. The following microsphere injection increased the differential pressure from 0.13 psi to 1.7 psi. As with the previous test, almost no oil was produced during the 1 PV microsphere injection. The oil bank appeared in the post-HSW injection. The oil production increased by 7.0% at the end of the post-water injection.

As shown in the results, the oil production of the microsphere in SmartWater 2 was higher than that in SmartWater 1. The possible reason was the differential pressure. After the waterflooding, the oil was mainly left in the small pores or low permeability zones due to the oil-wet nature of carbonate cores. The microsphere retention blocked the large pores and diverted the water phase to the small pores or low permeability zone bearing remaining oil. The high differential pressure could overcome the capillary pressure in these zones and promote the oil production. The maximum differential pressure of the microsphere injection in SmartWater 2 was 3.5 times higher than the value in SmartWater 1. This came from the swelling of the microsphere.

The lower brine salinity induced microsphere hydration and swelling more quickly. The swollen microsphere was much easily strained by the pores due to the steric effect. Moreover, the hydration produced additional interaction between the microsphere and the brine/rock. More energy dissipated when the microsphere flowed forward. All these made the differential pressure increase in the low salinity SmartWater 2 and produce more oil. It can be noted that the differential pressure decreased in the post-water injection in Test 5.

As previously mentioned, the swelling of the microsphere may be reversible in the high salinity brine. This may drive the microsphere forward to the deep position and mobilize the oil therein. The improved suspension stability by the low salinity water could also help the deep migration of the microsphere. The microsphere was observed in the produced fluid in both tests, which confirmed the deep migration of the microsphere in the salinity variation condition.

The oil bank appeared hysteretically at the post-water injection stage rather than at the breakthrough of the microsphere, which was different from the fractional flow theory. The polymer injection and microsphere injection are comparable with each other in the increasing differential pressure. The polymer thickened the water phase and slightly decreased the water permeability,

Fig. 6 *The oil production and differential pressure in Test 4.*

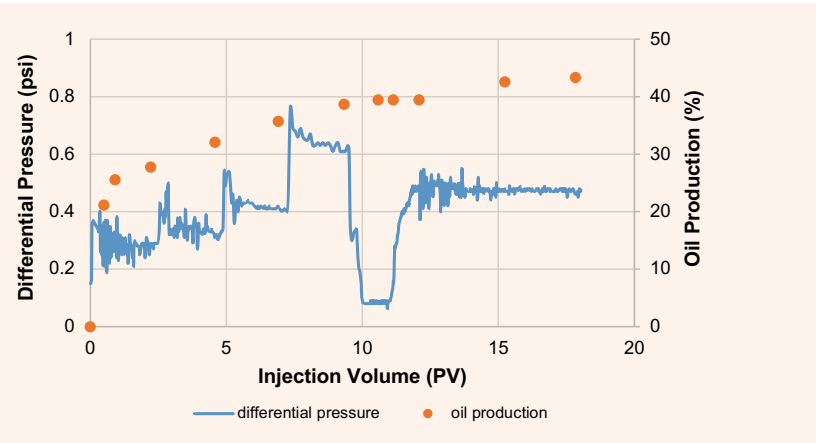

Fig. 7 *The oil production and differential pressure in Test 5.*

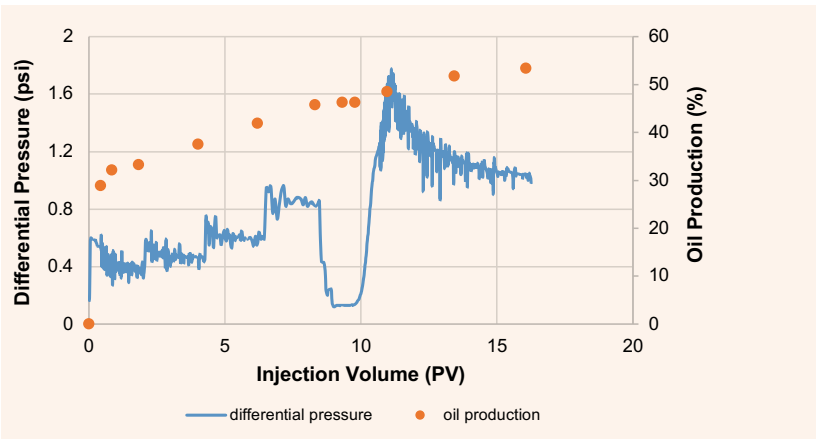

which resulted in a higher oil fractional flow than the waterflooding at the same water saturation. A shock or oil bank formed at the polymer front, due to the velocity difference of the saturation waves. The oil produced along with the polymer breakthrough. The microsphere injection seems not to follow the same physics given to the hysteretic oil bank.

The fractional flow theory applies only to the homogeneous media to the fluids. Although the cores were not ideally homogeneous, it could be taken as homogeneous because the polymer played the same role to the different

parts. Moreover, the effects of the microsphere to different permeability parts were not identical. The microsphere selectively entered the high permeability parts due to the size exclusion and partially block them. Water flow was diverted to the low permeability part. The flow rates in the low permeability parts were increased and the oil could be displaced out. When the oil flowed forward to the outlet, it was not speeded up as in the polymer case, therefore, the oil bank lagged behind the microsphere.

Conclusions

The bulk properties of the microsphere showed strong salinity dependency. The particle size of the microsphere increased from 0.25 µm in the injection water to a maximum 0.67 µm in the SmartWater with a lower strength. The zeta potential of the microsphere increased from -4.5 mV to -20.1 mV in the low salinity SmartWater.

The microsphere in the SmartWater produced a higher differential pressure in the carbonate core than in the injection water, but the maximum differential pressure after a chase of SmartWater injection was lower. There was a differential pressure response during the switch of the water salinity.

The microsphere in the low salinity SmartWater 2 produced more oil than in SmartWater 1 after waterflooding in the carbonate cores. The oil bank appeared hysteretically in the post-water injection stage in both tests. The microsphere was observed in the produced fluid due to the particle size change and the improved suspension stability of the microsphere in SmartWater.

References

1. Al-Yousef, A.A., Al-Saleh, S., Al-Kaabi, A.U. and Al-Jawfi, M.S.: "Laboratory Investigation of the Impact of Injection Water Salinity and Ionic Content on Oil Recovery from Carbonate Reservoirs," *SPE Reservoir Evaluation & Engineering*, Vol. 14, Issue 5, October 2011, pp. 578-593.
2. Al-Yousef, A.A., Al-Saleh, S. and Al-Jawfi, M.S.: "Improved/Enhanced Oil Recovery from Carbonate Reservoirs by Tuning Injection Water Salinity and Ionic Content," SPE paper 154076, presented at the SPE Improved Oil Recovery Symposium, Tulsa, Oklahoma, April 14-18, 2012.
3. Alotaibi, M.B., Nasralla, R.A. and Nasr-El-Din, H.A.: "Wettability Challenges in Carbonate Reservoirs," SPE paper 129972, presented at the SPE Improved Oil Recovery Symposium, Tulsa, Oklahoma, April 24-28, 2010.
4. Al-Yousef, A.A., Al-Saleh, S. and Al-Jawfi, M.S.: "SmartWater Flooding for Carbonate Reservoirs: Salinity and Role of Ions," SPE paper 141082, presented at the SPE Middle East Oil and Gas Show and Conference, Manama, Kingdom of Bahrain, September 25-28, 2011.
5. Ahmadi, A. and Moosavi, M.: "Investigation of the Effects of Low-Salinity Waterflooding for Improved Oil Recovery in Carbonate Reservoir Cores," *Energy Sources, Part A: Recovery, Utilization, and Environmental Effects*, Vol. 40, Issue 9, April 2018, pp. 1035-1043.
6. Seccombe, J.C., Lager, A., Webb, K.J., Jerauld, G., et al.: "Improving Waterflood Recovery: LoSalTM EOR Field Evaluation," SPE paper 113480, presented at the SPE Symposium on Improved Oil Recovery, Tulsa, Oklahoma, April 20-23, 2008.
7. Chen, Y., Xie, Q., Sari, A., Brady, P.V., et al.: "Oil/Water/Rock Wettability: Influencing Factors and Implications for Low Salinity Water Flooding in Carbonate Reservoirs," *Fuel*, Vol. 215, March 2018, pp. 171-177.
8. Sharma, H. and Mohanty, K.K.: "An Experimental and Modeling Study to Investigate Brine-Rock Interactions during Low Salinity Water Flooding in Carbonates," *Journal of Petroleum Science and Engineering*, Vol. 165, June 2018, pp. 1021-1039.
9. Zahid, A., Shapiro, A.A. and Skauge, A.: "Experimental Studies of Low Salinity Water Flooding Carbonate Reservoirs: A New Promising Approach," SPE paper 155625, presented at the SPE EOR Conference at Oil and Gas West Asia, Muscat, Oman, April 16-18, 2012.
10. Xie, Q., Sari, A., Pu, W., Chen, Y., et al.: "pH Effect on Wettability of Oil/Brine/Carbonate System: Implications for Low Salinity Water Flooding," *Journal of Petroleum Science and Engineering*, Vol. 168, September 2018, pp. 419-425.
11. Ayirala, S.C., Al-Yousef, A.A., Li, Z. and Xu, Z.: "Water Ion Interactions at Crude Oil-Water Interface: A New Fundamental Understanding on SmartWater Flood," *SPE Journal*, Vol. 23, Issue 5, October 2018.
12. Ayirala, S.C., Li, Z., Saleh, S.H., Xu, Z., et al.: "Effects of Salinity and Individual Ions on Crude Oil/Water Interface Physicochemical Interactions at Elevated Temperature," *SPE Reservoir Evaluation & Engineering*, Vol. 22, Issue 3, August 2019, pp. 897-910.
13. Ayirala, S.C., Saleh, S., Enezi, S. and Al-Yousef, A.A.: "Multiscale Aqueous-Ion Interactions at Interfaces for Enhanced Understanding of Controlled-Ionic-Composition-Waterflooding Processes in Carbonates," *SPE Reservoir Evaluation & Engineering*, Vol. 23, Issue 3, August 2020, pp. 1118-1132.
14. Al-Yousef, A.A., Liu, J.S., Blanchard, G.W., Saleh, S., et al.: "SmartWater Flooding: Industry's First Field Test in Carbonate Reservoirs," SPE paper 159526, presented at the SPE Annual Technical Conference and Exhibition, San Antonio, Texas, October 8-10, 2012.
15. Al-Sofi, A.M., Wang, J., Al-Boqmi, A.M., Al-Otaibi, M.B., et al.: "SmartWater Synergy with Chemical EOR for a Slightly Viscous Arabian Heavy Reservoir," SPE paper 184163, presented at the SPE Heavy Oil Conference and Exhibition, Kuwait City, Kuwait, December 6-8, 2016.
16. Al-Ghamdi, A., Ayirala, S.C., Al-Otaibi, M. and Al-Yousef, A.A.: "SmartWater Synergy with Surfactant Chemicals: An Electro-Kinetic Study," SPE paper 197239, presented at the Abu Dhabi International Petroleum Exhibition and Conference, Abu Dhabi, UAE, November 11-14, 2019.
17. Karimov, D., Hashmet, M.R. and Pourafshary, P.: "A Laboratory Study to Optimize Ion Composition for the Hybrid Low Salinity Water/Polymer Flooding," OTC paper 30136, presented at the Offshore Technology Conference Asia, Kuala Lumpur, Malaysia, November 2-6, 2020.
18. Alhuraishawy, A.K., Imqam, A., Wei, M. and Bai, B.: "Coupling Low Salinity Water Flooding and Preformed Particle Gel to Enhance Oil Recovery for Fractured Carbonate Reservoirs," SPE paper 180386, presented at the SPE Western Regional Meeting, Anchorage, Alaska, May 23-26, 2016.
19. Alhuraishawy, A.K., Wei, M., Bai, B. and Al-Mansour, A.: "Integrating Microgels and Low Salinity Waterflooding to Improve Conformance Control in Fractured Reser-

voirs," SPE paper 188384, presented at the Abu Dhabi International Petroleum Exhibition and Conference, Abu Dhabi, UAE, November 13-16, 2017.

20. Alhuraishawy, A.K. and Bai, B.: "Evaluation of Combined Low Salinity Water and Microgel Treatments to Improve Oil Recovery Using Partial Fractured Carbonate Models," *Journal of Petroleum Science and Engineering*, Vol. 158, September 2017, pp. 80-91.
21. Alhuraishawy, A.K., Bai, B., Wei, M., Al-Mansour, A., et al.: "Integrating Microgel-Low Salinity Waterflooding to Improve Production Profile in Non-Crossflow Heterogeneous Reservoir," SPE paper 192154, presented at the SPE Kingdom of Saudi Arabia Annual Technical Symposium and Exhibition, Dammam, Saudi Arabia, April 23-26, 2018.
22. Alhuraishawy, A.K., Bai, B. and Wei, M.: "Combined Ionically Modified Seawater and Microgels to Improve Oil Recovery in Fractured Carbonate Reservoirs," *Journal of Petroleum Science and Engineering*, Vol. 162, March 2018, pp. 434-445.
23. Brattekås, B., Graue, A. and Seright, R.S.: "Low Salinity Chase Waterfloods Improve Performance of Cr(III)-Acetate Hydrolyzed Polyacrylamide Gel in Fractured Cores," SPE paper 173749, presented at the SPE International Symposium on Oil Field Chemistry, The Woodlands, Texas, April 13-15, 2015.
24. Brattekås, B. and Seright, R.: "The Mechanism for Improved Polymer Gel Blocking during Low Salinity Waterfloods, Investigated Using Positron Emission Tomography Imaging," *Transport in Porous Media*, Vol. 133, May 2020, pp. 119-138.
25. Liu, C., Liao, X., Zhang, Y., Chang, M-M., et al.: "Field Application of Polymer Microspheres Flooding: A Pilot Test in Offshore Heavy Oil Reservoir," SPE paper 158295, presented at the SPE Annual Technical Conference and Exhibition, San Antonio, Texas, October 8-10, 2012.
26. Cai, Y., Li, X., Shi, M., Yang, L., et al.: "Research on the Adaptability of Polymeric Nanosphere Flooding in Extra-low Permeability Reservoir in Changing Oil Fields," *Oil Drilling and Production Technology*, Vol. 35, Issue 4, 2013, pp. 88-93.
27. Cao, D., Han, M., Wang, J. and Al-Sofi, A.: "Optimization of Microsphere Injection by Balancing the Blocking and Migration Capacities in a Heterogeneous Carbonate Matrix," SPE paper 203131, presented at the Abu Dhabi International Petroleum Exhibition and Conference, Abu Dhabi, UAE, November 9-12, 2020.
28. Bai, B., Zhou, J. and Yin, M.: "A Comprehensive Review of Polyacrylamide Polymer Gels for Conformance Control," *Petroleum Exploration and Development*, Vol. 42, Issue 4, August 2015, pp. 525-532.
29. Zaitoun, A., Makakou, P., Blin, N., Al-Maamari, R.S., et al.: "Shear Stability of EOR Polymers," *SPE Journal*, Vol. 17, Issue 2, June 2012, pp. 335-339.
30. Zhang, X., Han, M., Fuseni, A. and Al-Sofi, A.M.: "An Approach to Evaluate Polyacrylamide-type Polymers' Long-term Stability under High Temperature and High Salinity Environment," *Journal of Petroleum Science and Engineering*, Vol. 180, September 2019, pp. 518-525.

About the Authors

Dongqing Cao

M.S. in Petroleum Engineering, China University of Petroleum

Dongqing Cao joined the Aramco Beijing Research Center in July 2012 as a Petroleum Engineer. His research areas include physical modeling by coreflooding and micromodel, oil field chemicals for oil production, fluid diversion, and conformance control.

Dongqing has authored and coauthored 13 conference papers and journal papers, and published one patent.

He received both his B.S. and M.S. degrees in Petroleum Engineering from the China University of Petroleum, Qingdao, China.

Dr. Ming Han

Ph.D. in Chemistry, University of Rouen

Dr. Ming Han is a Petroleum Engineering Consultant in chemical enhanced oil recovery, working in Saudi Aramco's Exploration and Petroleum Engineering Center – Advanced Research Center (EXPEC ARC). Before joining Saudi Aramco in 2007, he worked for the China National Offshore Oil Corporation (CNOOC), where he was Lead Engineer in Oil Field Chemistry at the CNOOC Research Center working to implement an offshore polymer flooding project. For more than 10 years of his career, Ming worked for the Research Institute of Petroleum Exploration and Development (RIPED) in China as a Research Engineer, conducting laboratory studies and field pilots in water shutoff, profile modification, polymer flooding and chemical flooding. He also worked at Hycal Energy Research in Canada as a Research Engineer.

In 1982, Ming received his B.S. degree in Polymer Chemistry from Jilin University, Changchun, China. He received his M.S. degree from the University of Paris VI, Paris, France, and his Ph.D. degree from the University of Rouen, Mont-Saint-Aignan, France, both in Polymer Physico-Chemistry.

Ming is a member of the Society of Petroleum Engineers (SPE) and the American Chemical Society (ACS).

Salah H. Al Saleh

B.S. in Geochemistry,
King Abdulaziz University

Salah H. Al Saleh is a Petroleum Scientist with the Reservoir Engineering Technology Division of Saudi Aramco's Exploration and Petroleum Engineering Center – Advanced Research Center (EXPEC ARC). He has more than 30 years of specialized and research experience in conventional and special core analysis, capillary pressure and relative permeability by centrifuge, electrical properties, improved oil recovery (IOR)/enhanced oil recovery (EOR), including SmartWater flooding, chemical, thermal, and carbon dioxide techniques, assisted by imaging technologies such as X-ray computer tomography and nuclear magnetic resonance imaging.

Salah has received several awards during his career, including the King Salman prize for Innovation Award.

He has authored and coauthored 45 technical papers, 22 journal articles, and holds 12 U.S. patents and several pending patent applications.

Salah received his B.S. degree in Geochemistry from King Abdulaziz University, Jiddah, Saudi Arabia.

Dr. Subhash C. Ayirala

Ph.D. in Petroleum Engineering,
Louisiana State University

Dr. Subhash C. Ayirala is an Improved/Enhanced Oil Recovery (IOR/EOR) Specialist and is currently leading the SmartWater Flooding team at Saudi Aramco's Exploration and Petroleum Engineering Center – Advanced Research Center (EXPEC ARC), as the Focus Area Champion. He has more than 15 years of experience in the oil and gas industry.

Subhash played a major role in the successful execution of the SmartWater flooding multiscale research program, in addition to unraveling the importance of injection water chemistry in the EOR portfolio to develop several novel hybrid recovery technologies.

Prior to joining Saudi Aramco, he worked as a Reservoir Engineer in Shell International Exploration & Production, Houston, Texas. Subhash has authored or coauthored more than 70 technical papers, 50 journal publications, and holds 25 granted U.S. patents, and 10 pending patent applications.

He is a Society of Petroleum Engineers (SPE) distinguished member, and serves as co-executive editor for the SPE *Reservoir Evaluation & Engineering Journal*. Subhash also serves as one of the Executive Editors for the *Journal of Petroleum Science and Engineering* (JPSE), an Elsevier international journal. He received the SPE Outstanding Technical Editor recognition nine times in 2008, 2013, 2016, 2017, 2018, 2019, and 2020, and is the recipient of the 2017 SPE "A Peer Apart Award." Subhash also received the 2019 SPE Middle East and North Africa Regional Service Award.

Subhash received both his M.S. and Ph.D. degrees in Petroleum Engineering from Louisiana State University, Baton Rouge, LA. He also holds a B.Tech and an M.Tech degree in Chemical Engineering from Sri Venkateswara University, Titupati, and the Indian Institute of Technology, Kharagpur, India, respectively.

Dr. Ali A. Al-Yousef

Ph.D. in Petroleum Engineering,
University of Texas at Austin

Dr. Ali A. Yousef is a Senior Petroleum Engineering Consultant and Chief Technologist at the Reservoir Engineering Technology Division in Saudi Aramco's Exploration and Petroleum Engineering Center – Advanced Research Center (EXPEC ARC). He has more than 26 years of experience in upstream research and technology. Since joining Saudi Aramco, Ali has been involved in applied research projects on improved oil recovery (IOR), waterflooding, enhanced oil recovery (EOR), and advanced reservoir evaluation/monitoring. He played a pivotal role in planning, developing and implementing the EOR roadmap for the company.

Ali is currently leading more than 50 scientists, engineers, and technicians. Those researchers are dedicated to the development of various IOR/EOR processes, including SmartWater, CO_2, and chemical EOR technologies as well as other novel technologies focusing on nanotechnology and advanced reservoir evaluation/monitoring.

He has written over 100 technical papers, and has 32 granted patents and more than 30 pending patent applications. Ali is currently an active member of the Society of Petroleum Engineers (SPE) and has chaired several SPE workshops and forums, helped organize several petroleum engineering related conferences, and taught courses on IOR/EOR and waterflooding.

He is considered as a worldwide authority in the field of IOR/EOR. Ali was the recipient of SPE's prestigious IOR Pioneer Award at the 2016 IOR Conference in Tulsa for his significant contributions made to the advancement of recovery technologies.

He was recognized by The Custodian of the Two Holy Mosques in 2018 for his pioneering invention on SmartWater flooding technology. More recently, the technology on the zero liquid discharge (ZLD) water management solution that Ali co-invented has received the World Oil's 2020 Best Water Management Technology Award. He has also been elected as a 2021 Fellow of Energy Institute (FEI).

Ali received his B.S. degree in Chemical Engineering from King Fahd University of Petroleum and Minerals (KFUPM), Dhahran, Saudi Arabia, and his M.S. and Ph.D. degrees, both in Petroleum Engineering, from the University of Texas at Austin, Austin, TX.